# Coherent Operation of a Tunable Quantum Phase Gate in Cavity QED

A. Rauschenbeutel, G. Nogues, S. Osnaghi, P. Bertet, M. Brune, J. M. Raimond, and S. Haroche
*Laboratoire Kastler Brossel, Département de Physique de l'Ecole Normale Supérieure, 24 rue Lhomond, F-75231 Paris Cedex 05, France*
(Received 29 July 1999)

We have realized a quantum phase gate operating on quantum bits carried by a single Rydberg atom and a zero- or one-photon field in a high-$Q$ cavity. The gate operation is based on the dephasing of the atom-field state produced by a full cycle of quantum Rabi oscillation. The dephasing angle, conditioned to the initial atom-field state, can be adjusted over a wide range by tuning the atom-cavity frequency difference. We demonstrate that the gate preserves qubit coherence and generates entanglement. This gate is an essential tool for the nondestructive measurement of single photons and for the manipulation of many-qubit entanglement in cavity QED.

PACS numbers: 03.67.Lx, 32.80.Rm, 42.50.Ar

Entanglement is a most striking feature of quantum theory. Its puzzling implications have motivated an intense theoretical and experimental research work. It has been proposed to make use of many entangled two-level quantum systems (qubits) to implement new information processing functions [1]. These applications require the production of complex entangled states. Such manipulations can be decomposed into a sequence of simple unitary evolutions, involving one or two qubits, performed by quantum gates.

One of the simplest two-qubit gates is the conditional quantum phase gate (QPG) [2,3]. The QPG transformation simply reads

$$|a,b\rangle \rightarrow \exp(i\phi\,\delta_{a,1}\delta_{b,1})\,|a,b\rangle\,, \qquad (1)$$

where $|a\rangle, |b\rangle$ stand for the basis states ($|0\rangle$ or $|1\rangle$) of the two qubits and $\delta_{a,1}$, $\delta_{b,1}$ are the usual Kronecker symbols.

The QPG leaves the initial state unchanged, except if both qubits are 1, in which case the state is phase shifted by an angle $\phi$. This gate is universal, since any quantum computation can be realized by combining QPGs and rotations of individual qubits. For example, a $\pi$-shift QPG and appropriate rotations of the second qubit realize a controlled-NOT or XOR gate which performs the transformation [4],

$$|a,b\rangle \rightarrow |a, a \oplus b\rangle\,, \qquad (2)$$

where $\oplus$ represents the addition modulo two.

The experimental realization of these fundamental gates has led recently to considerable experimental efforts. Liquid sample NMR experiments [5] use as qubits nuclear spins in macroscopic ensembles of molecules. The information is extracted out of the small departure of these systems from thermal equilibrium. Simple demonstrations have been realized, but these devices do not generate clear-cut entanglement [6] and are not scalable to large numbers of independent qubits. Moreover, a quantum measurement of individual qubits, an essential ingredient in quantum algorithms, is not possible.

In quantum optics experiments with atoms, photons, or trapped ions, qubits are individually addressed. Conditional phase shifts involving atom and photon [3,7] as well as two-atom entanglement [8,9] have been demonstrated in cavity QED and ion-trap experiments. A XOR gate with a single ion has been realized [10] but qubit entanglement has not been directly checked on this gate.

We report here the operation of a QPG using as qubits a zero- or one-photon field and a single Rydberg atom. We adjusted the $\phi$ angle of Eq. (1) between 54° and 273°, over a range much wider than in previous cavity-QED conditional phase shift devices [3,7]. We have operated the QPG with initial qubits prepared in state superpositions, thus producing an entangled qubit output, studied experimentally in detail. This gate, whose present performances and limitations are analyzed, is essential for the nondestructive measurement of a single photon [11]. It is also a promising tool for engineering entanglement of many qubits.

Our experimental setup [11–13] is depicted in Fig. 1. The three relevant atomic circular Rydberg states with principal quantum numbers $n = 51$ ($e$ in the following), $n = 50$ ($g$), and $n = 49$ ($i$) are shown in the inset of Fig. 1. The atoms, effusing from oven $O$, are velocity selected by laser optical pumping and prepared in state $e$ or $g$ by laser and radio frequency excitation [14] in zone $B$. They cross one at a time the cavity $C$ sustaining a Gaussian field mode (waist $w = 6$ mm), resonant or

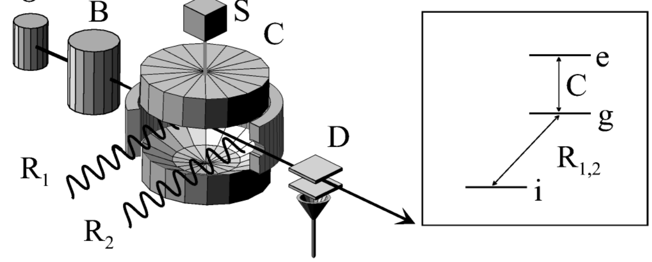


FIG. 1. Scheme of cavity-QED QPG gate with relevant atomic energy levels in the inset.

 0031-9007/99/83(24)/5166(4)$15.00 

nearly resonant with the $e \rightarrow g$ transition at 51.1 GHz. This cavity is made of two superconducting niobium mirrors enclosed by an aluminum ring with small holes for atom access (the ring is cut open in the figure to show the inside of $C$).

The atom and field relaxation times, 30 and 1 ms, respectively, are long enough to permit a coherent operation of the gate (atom-cavity interaction time $t$ around 20 $\mu$s).

The atomic preparation is pulsed, so that the position of each atom is known within $\pm 1$ mm. The atoms are detected, after $C$, by a state selective field-ionization detector $D$ which discriminates between $e$, $g$, and $i$. The field is injected in $C$ either by an external coherent source $S$ or by a "source" atom crossing $C$ before the atomic qubit. The whole setup is cooled to 1.3 K. The mean number of thermal photons in $C$, dominated by microwave leaks, is 0.7. Radiation cooling is provided, before each experimental sequence, by pulses of atoms crossing $C$ in level $g$. They absorb the residual thermal field. This cooling reduces the background to 0.12 photon on average [11].

The gate acts on the atomic levels $i$ and $g$ (0 and 1 for the atomic qubit), and on zero- and one-photon states. If the atom is in the uncoupled level $i$ or if the cavity is empty ($\delta_{a,1}\delta_{b,1} = 0$), the atom-field state is unchanged as required by Eq. (1). Finally, $|g, 1\rangle$ should evolve into $\exp(i\phi)|g, 1\rangle$ to fulfill Eq. (1) when $\delta_{a,1}\delta_{b,1} = 1$. This is achieved by the completion of a full-cycle Rabi oscillation between the initial state $|g, 1\rangle$ and the auxiliary state $|e, 0\rangle$ while the atom crosses $C$. At resonance, a $2\pi$ Rabi pulse transforms $|g, 1\rangle$ into $-|g, 1\rangle = \exp(i\phi)|g, 1\rangle$, with $\phi = \pi$. It is realized by setting the atomic velocity to $v = 503$ (2.5) m/s. The effective atom-field interaction time $t = \sqrt{\pi}\, w/v$ is then such that $\Omega t = 2\pi$ where $\Omega/2\pi = 47$ kHz is the corresponding Rabi frequency [12]. The $\pi$ phase shift of the atom-field wave function, also used in [10], is analogous to the sign change of a spin 1/2 state undergoing a $2\pi$ rotation [15]. Note also that $2\pi$ Rabi pulses, leaving the field unchanged, are essential for the generation of "trapping states" in a micromaser [16].

In order to realize a QPG with a different $\phi$ angle, we detune the cavity mode from the $e \rightarrow g$ transition frequency by an amount $\delta$, without changing the atomic velocity. Numerical simulations show that the tip of the Bloch vector, representing the system in the $\{|g, 1\rangle, |e, 0\rangle\}$ basis, evolves, from $|g, 1\rangle$, on an almost *closed* trajectory on the Bloch sphere. The accumulated phase $\phi$ varies between 0 and $2\pi$ when $\delta$ is swept across 0. The final absorption of the photon is prevented at resonance by the $2\pi$ pulse condition and, far from resonance, by energy conservation. For intermediate $\delta$ values of the order of $\Omega$ the theoretical absorption rate remains below 3%. This remarkable result is due to the smooth variation of the atom-field coupling when the atom crosses the Gaussian mode.

This theoretical residual absorption rate could even be completely suppressed by slightly adjusting the atomic velocity for each $\delta$ value.

To check the operation of our QPG, we send the atomic qubit in the state superposition $(1/\sqrt{2})(|i\rangle + |g\rangle)$ through $C$ containing either zero or one photon. This superposition should ideally become $(1/\sqrt{2})[|i\rangle + \exp(i\phi)|g\rangle]$ if there is one photon in $C$, while it is left unaltered if $C$ is empty. We use a Ramsey separated oscillatory field interferometer [17] to prepare and probe the $g$-$i$ superposition: auxiliary microwave pulses $R_1$ and $R_2$, nearly resonant with the $g \rightarrow i$ transition at 54.3 GHz, are applied to the atoms before and after they cross the Gaussian cavity mode.

These pulses are fed into the cavity-ring structure through a small hole in the ring (not shown in Fig. 1). Their timing relies on the precise knowledge of each atom's position. The atoms, initially in $g$, are prepared in the proper state by the pulse $R_1$. After the atom has crossed $C$, the superposition is analyzed by applying the $\pi/2$ pulse $R_2$ to the atom before detecting it in $g$ or $i$. We reconstruct, as a function of the frequency $\nu$ of the $R_1$ and $R_2$ pulses, the probability $P_g$ for finding the atom in $g$. This signal exhibits the sinusoidal modulation known as "Ramsey fringes."

To record the fringes corresponding to one photon in $C$ we send a source atom through $C$ before the atomic qubit. The source is initially in $e$ and undergoes no Ramsey pulses. Its resonant interaction time with $C$ is adjusted to the value corresponding to a $\pi$ Rabi pulse by Stark tuning the transition out of the cavity resonance at the proper time using a time-varying electric field applied across the mirrors [13]. When the source is properly detected in $g$, $C$ stores one photon. Events in which the source is spuriously detected in $e$ are rejected.

The single-photon fringes on the qubit atom are shown in Figs. 2(a)–2(c) (solid squares), for three values of the atomic qubit-cavity detuning ($\delta/2\pi = 22$, 0, and $-15.5$ kHz). In each case, the fringes corresponding to an empty cavity, obtained by removing the source, are shown for reference (open diamonds).

The difference between the phases of the sinusoidal fits to the square and diamond fringes (lines in Fig. 2) yields $\phi = 273°$, 179°, and 94° for 2(a), 2(b), and 2(c), respectively. Figure 3 displays the measured phase $\phi$ versus $\delta$. The points are experimental and the line results from a numerical calculation taking into account the system's imperfections. The agreement with the experiment is very good.

This experiment shows the continuous evolution of the phase shift from the resonant case ($\phi = \pi$), to the nonresonant, dispersive one. We have also determined the residual absorption rate of our QPG (ideally equal to zero): we measured, as a function of $\delta$, the probability for finding the atomic qubit in level $e$ when there is one photon in $C$, the pulses $R_1$ and $R_2$ being switched

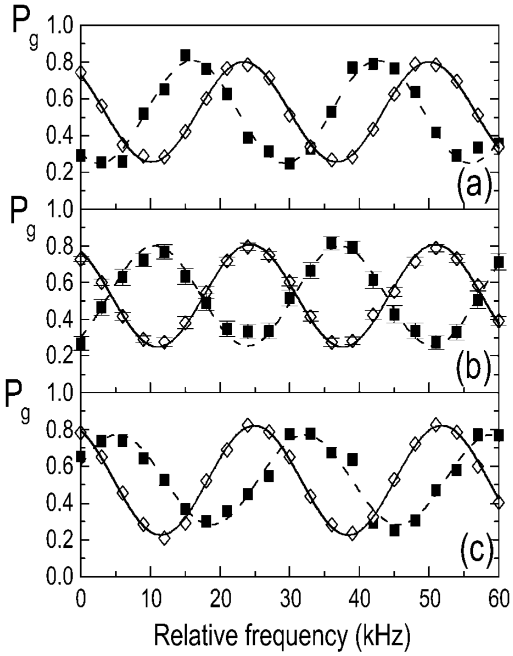


FIG. 2. Probability $P_g$ to detect the atom in state $g$ versus $\nu$ for various atom-cavity detunings $\delta/2\pi = 22$, 0, and $-15.5$ kHz in (a), (b), and (c), respectively. Statistical error bars are shown for (b). Lines are sine fits and points are experimental (open diamonds: empty cavity; solid squares: single-photon fringes).

off. This absorption rate is about 20% and indicates the present limitations of the gate (imperfections of the $2\pi$ Rabi pulse, effect of residual thermal fields, cross talk between the detection channels, etc.). The main contribution to the absorption at resonance ($\delta = 0$) is due to the 0.12 probability for having one photon in $C$ before the source enters it. In this case, the source adds a second photon and the atomic qubit experiences a Rabi rotation

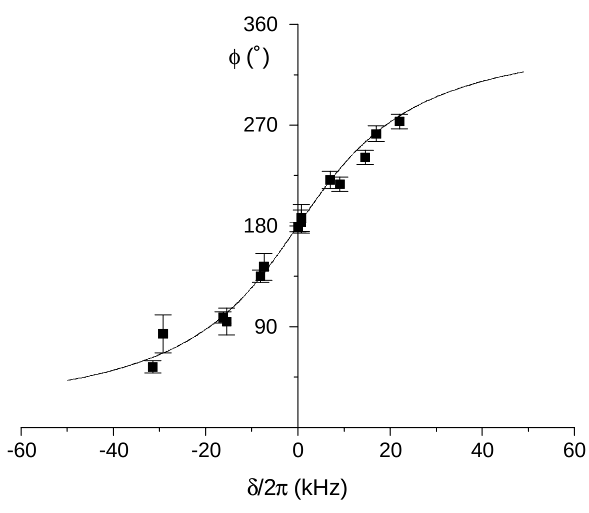


FIG. 3. Conditional phase shift versus $\delta/2\pi$. The line is a theoretical fit.

angle $\Omega\sqrt{2}\,t = 2\sqrt{2}\,\pi$, close to $3\pi$. The atomic qubit then ends up in level $e$ with a probability close to 1.

In order to demonstrate that our QPG generates entanglement, we finally operate it with both input qubits in a state superposition. The atomic qubit state, $(1/\sqrt{2})\,(|i\rangle + |g\rangle)$, is produced, as above, by a $\pi/2$ pulse $R_1$ (no $R_2$ pulse is applied). The field qubit superposition, $c_0|0\rangle + c_1|1\rangle$, is generated by injecting into $C$ a small coherent field (average number of photons $n_0 = 0.18$). For that purpose, the source $S$ is coupled to $C$ during a 10 $\mu$s time interval. The exact state of the field (amplitude $\alpha = \sqrt{n_0}$) writes $|\alpha\rangle = c_0|0\rangle + c_1|1\rangle + \sum_{n>1} c_n|n\rangle$ with $c_0 = 1 - n_0/2 = 0.91$, $c_1 = \sqrt{n_0} = 0.4$, and $c_n$ negligible for $n > 1$. To a good approximation it is thus a superposition of zero- and one-photon states. The initial product state of the two qubits, $(1/\sqrt{2})\,(|i\rangle + |g\rangle)\,(c_0|0\rangle + c_1|1\rangle)$, is transformed by the gate operation into an entangled state $|\Psi\rangle$ which can be expressed in two equivalent forms:

$$|\Psi\rangle = \{c_0|0\rangle(|i\rangle + |g\rangle) + c_1|1\rangle(|i\rangle + e^{i\phi}|g\rangle)\}/\sqrt{2}\,, \tag{3}$$

$$= \{|i\rangle(c_0|0\rangle + c_1|1\rangle) + |g\rangle(c_0|0\rangle + e^{i\phi}c_1|1\rangle)\}/\sqrt{2}\,. \tag{4}$$

Equations (3) and (4) exhibit the symmetry of the QPG: either the field in state one can be considered as the control qubit which produces a phase shift of the atom in state $g$ [Eq. (3)] or, conversely, the atom in $g$ is the control qubit which dephases the one-photon state Eq. (4)].

The correlations implied by Eq. (3) have already been demonstrated. We showed above that the phase of the atomic coherence is correlated to the photon number in $C$. In order to verify the correlations described by Eq. (4), we analyze the phase of the field in $C$ by means of a "homodyning" method: we inject, after the atom has left $C$, a field with the amplitude $\alpha\exp(i\theta)$. It adds coherently to the field already present in $C$. The phase $\theta = T\Delta\nu$ depends upon the detuning $\Delta\nu$ between $S$ and $C$ ($T = 100$ $\mu$s is the delay between the two field injections). The amplitude of the resulting field ideally varies between 0 and $2\alpha$ as a function of the phase difference between the homodyning pulse and the field left in $C$ after the interaction with the atomic qubit. In this experiment, we set the atom-cavity detuning $\delta$ to zero ($\phi = \pi$) and vary the phase $\theta$ by sweeping the frequency of $S$.

The final field is probed by sending an atom, initially in $g$, across $C$ ($R_1$ and $R_2$ are switched off). This probe atom undergoes a $\pi$ Rabi pulse in the field of one photon. Hence, the probability $P(e)$ for detecting it in $e$ is ideally equal to the probability for finding a single photon in $C$ (the latter being approximately the average photon number).

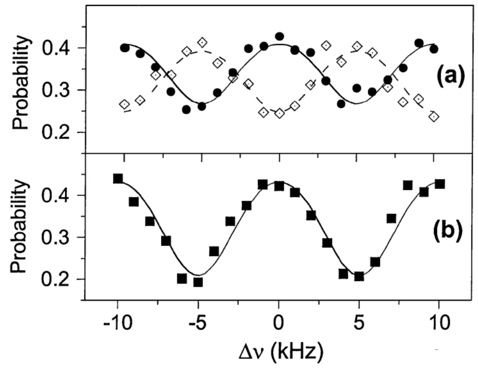


FIG. 4. Probing qubit entanglement: a small coherent field (amplitude $\alpha = \sqrt{0.18}$) is used as *field* qubit. The atomic qubit, initially in $g$, crosses $R_1$ and $C$, before being detected. A homodyning field $\alpha \exp(i\Delta\nu T)$ is then added in $C$. A last atom initially in $g$ probes the final field. (a) Conditional probabilities $P(e/i)$ (circles) and $P(e/g)$ (diamonds) versus $\Delta\nu$ to detect the probe in $e$ if the atomic qubit has crossed $C$ in $i$ or $g$. (b) Probability $P(e)$ to detect the probe in $e$ without atomic qubit. Points are experimental and lines are fits based on a simple model.

Figure 4(a) shows the conditional probabilities $P(e/i)$ and $P(e/g)$ for finding the probe in $e$ provided the atomic qubit was found in $i$ (circles) or in $g$ (diamonds) versus $\Delta\nu$. The lines are obtained by a simple model which accounts for the experimental imperfections by adjustable contrasts and offsets. As a control, we show [Fig. 4(b)] $P(e)$ versus $\Delta\nu$ when no atomic qubit is sent across $C$. In this case, the probe absorption is maximum for $\Delta\nu = 0$ since the amplitudes of the two injected fields then add with the same phase. The modulation of $P(e)$ when $\Delta\nu$ is tuned reflects the interference of these two fields when they have different phases. The signals in Fig. 4(a) clearly exhibit the phase correlations of Eq. (4): the atomic qubit in $i$ leaves the field phase unchanged [the line with the circles in Fig. 4(a) has the same phase as the line in Fig. 4(b)] while the atomic qubit in $g$ shifts the phase of the field by $\pi$ [the line with the diamonds in Fig. 4(a) has a phase opposite to the line in Fig. 4(b)].

The phase correlations shown in Figs. 2 and 4 prove that our cavity-QED QPG operates in a symmetrical and coherent way. It generates the expected output qubit entanglement when the input qubits are in state superpositions. Each qubit has, in its "active" one state, an adjustable dephasing effect on the corresponding state of the other qubit. Apart from this dephasing, the qubit states are, at resonance, with a 0.9 probability, unaltered by the gate. This fidelity could be increased by optimizing the Rabi pulse contrast, decreasing the thermal field background and improving the discrimination of the atomic detectors.

Our QPG has many interesting applications. Combined with the $R_1$-$R_2$ Ramsey interferometer set to a fringe extremum, the QPG with $\phi = \pi$ is equivalent to a XOR gate in which the photon plays the role of the control qubit: the photon state determines the final atomic state, which stays unchanged if there is zero photon, and which switches (e.g., from $g$ to $i$) if there is one photon in $C$. A detection of the final atom state hence amounts to a nondestructive measurement of a single-photon field. We carried out this experiment which is described in [11]. The QPG could also be used to manipulate entanglement in many-atom systems. In [8], we describe an experiment in which a single-photon field is used as a "catalyst" to entangle two atoms in an (Einstein-Podolosky-Rosen) EPR-like pair [18]. A third atom, sent across the cavity between the two atoms of this pair can be used to manipulate, via the QPG operation, the phase of this transient cavity field. This makes it possible to control the relative phase of the two components of the EPR pair state. This experiment, under way in our laboratory, is equivalent to the preparation of a triplet of entangled atoms of the Greenberger-Horne-Zeilinger type [19].

We acknowledge support of the European Community.

[1] D. P. DiVincenzo, Science **270**, 255 (1995); A. Ekert and R. Josza, Rev. Mod. Phys. **68**, 3733 (1997).
[2] S. Lloyd, Phys. Rev. Lett. **75**, 346 (1995).
[3] Q. A. Turchette *et al.*, Phys. Rev. Lett. **75**, 4710 (1995).
[4] A. Barenco *et al.*, Phys. Rev. Lett. **74**, 4083 (1995).
[5] N. A. Gershenfeld and I. L. Chuang, Science **275**, 350 (1997); D. G. Cory, A. F. Fahmy, and T. F. Havel, Proc. Natl. Acad. Sci. U.S.A. **94**, 1634 (1997); J. A. Jones, M. Mosca, and R. H. Hansen, Nature (London) **393**, 344 (1998); D. G. Cory *et al.*, Phys. Rev. Lett. **81**, 2152 (1998).
[6] S. L. Braunstein *et al.*, Phys. Rev. Lett. **83**, 1054 (1999).
[7] M. Brune *et al.*, Phys. Rev. Lett. **72**, 3339 (1994).
[8] E. Hagley *et al.*, Phys. Rev. Lett. **79**, 1 (1997).
[9] Q. A. Turchette *et al.*, Phys. Rev. Lett. **81**, 3631 (1998).
[10] C. Monroe *et al.*, Phys. Rev. Lett. **75**, 4714 (1995).
[11] G. Nogues *et al.*, Nature (London) **400**, 239 (1999).
[12] M. Brune *et al.*, Phys. Rev. Lett. **76**, 1800 (1996).
[13] X. Maître *et al.*, Phys. Rev. Lett. **79**, 769 (1997).
[14] P. Nussenzveig *et al.*, Phys. Rev. A **48**, 3991 (1993).
[15] H. Rauch *et al.*, Phys. Lett. **54A**, 425 (1975); S. A. Werner *et al.*, Phys. Rev. Lett. **35**, 1053 (1975).
[16] M. Weidinger *et al.*, Phys. Rev. Lett. **82**, 3795 (1999).
[17] N. F. Ramsey, *Molecular Beams* (Oxford University Press, New York, 1985).
[18] A. Einstein, B. Podolosky, and N. Rosen, Phys. Rev. **47**, 777 (1935).
[19] D. M. Greenberger, M. A. Horne, and A. Zeilinger, Am. J. Phys. **58**, 1131 (1990); S. Haroche, in *Fundamental Problems in Quantum Theory*, edited by D. Greenberger and A. Zeilinger (New York Academy of Sciences, New York, 1995), Vol. 755, p. 73.